Journal of Applied and Computational Mechanics, Vol. 1, No. 2, (2015), 83-94
DOI: 10.22055/jacm.2014.10766

Journal of
Applied and Computational Mechanics

Investigation the effects of injection pressure and compressibility and nozzle entry in diesel injector nozzle's flow

Seyedmohammadjavad Zeidi[1], Miralam Mahdi[2]

[1]Undergraduate student, Mechanical Engineering Department, Shahid Rajaee Training Teacher University
Karaj, Tehran, 3198636886, IRANMohammadjavad313@gmail.com,
[2] Assistant Professor, Mechanical engineering Department, Shahid Rajaee Training Teacher University
Tehran, Postal Code, IRAN, M.mahdi@srttu.edu

Received April 21 2014; revised August 29 2014; accepted for publication August 29 2014.
Corresponding author: Miralam mehdi, M.mahdi@srttu.edu

Abstract

Investigating nozzle's orifice flow is challenging both experimentally and theoretically. This paper focuses on simulating flow inside diesel injector nozzle via Ansys fluent v15. Validation is performed with experimental results from Winkhofler et al (2001). Several important parameters such as mass flow rate, velocity profiles and pressure profiles are used for this validation. Results include the effects of contraction inside nozzle's orifice, effect of compressibility; effect of injection pressures and several orifice entries are also simulated in this study. To consider the effect of compressibility, a user defined function used in this simulation. The Cavitation model which is used in this simulation is Singhal et al. (2002) cavitation model. Presto discretization method is used for Pressure equation and second upwind discretization method is used for Momentum equation. Converging Singhal et al. cavitation model is very challenging and it needs several efforts and simulations.

Keywords: Two phase flow, Mass flow rate, Nozzle entry, Cavitation, Singhal

1. Introduction

The cavitation phenomenon is the formation of vapor or gas cavities within a given liquid driven by pressure change without any heating. It can be interpreted as the rupture of the liquid continuum due to excessive stresses. The liquid to vapor transition may be obtained either by heating the liquid at constant pressure, which is well known as boiling, or by decreasing the pressure in the liquid at constant temperature, which corresponds to the cavitation phenomena. It is commonly admitted that cavitation occurs at a given temperature T whenever the pressure p in the liquid becomes lower than the saturated vapor pressure $p_v(T)$, namely $p(T) \le p_v(T)$ [1].

The important features of atomization, including the size of the initial droplets and the fragmentation processes, are mainly governed by the flow in the nozzle [2] which ejects the spray. It is therefore important to study the flow inside the nozzle to find out how it is linked to the flow in the combustion cylinder. Experimental studies of cavitation flows in nozzles and orifices and also flows around bodies of different shapes have revealed a relationship between the cavitation number and the extent of the cavitation region. This has resulted in classification of cavitation flow regimes depending on the cavitation number, namely: *incipient*, *developed* (sub-cavitation and transitional cavitation), and *super-cavitating* [3, 4]. Significant progress in clarification of the structure of cavitation flows in nozzles has been achieved:

Bergwerk showed that variation of cavitation pattern can influence jet formation [5], Winklhofer et al. studied the formation of cavitation phenomena with changing outlet pressure with different diagram [6].

Martynov also investigated the effect of number of bubble nuclea and initial mass fraction on the vapor field for inlet cavitation [7]. Several cavitation models have been introduced ever since, such as Schnerr and Sauerr cavitation model, Zwart gerber belamri cavitation model, Singhal cavitation model [8]. In this study, Singhal et al. cavitation

model will be used which considers the effect of noncondensable gas [9]. Cavitation inception can be caused by "geometrical" and "dynamic" factors [10]. The first step of this study is to validate present simulation with Winklhofer et al. experiment [6]. Then, it is intended to investigate the effect of compressibility on flow inside orifice which is necessary to discern the differences. In the next scope, four different orifice entry are used for simulations and at end of simulations the best entry is chosen. In this study, injection pressure is high enough for comparing with real injecting condition.

2. Governing equations

The governing equations for a two-phase flow in this study are based on a single-fluid approach, regarding the mixture as one liquid referred to as "Mixture Model" in ANSYS FLUENT V 14. The flow field is then solved for the mixture continuity and momentum equations,

$$\frac{\partial}{\partial t}(\rho_m)+\nabla.(\rho_m\vec{v})=0 \tag{1}$$

$$\frac{\partial}{\partial t}(\rho_m)+\nabla.(\rho_m\vec{v})=-\nabla p+\nabla.\left[\mu_m\left(\nabla\vec{v}+\nabla\vec{v}^{T}\right)\right]+\rho_m\vec{g} \tag{2}$$

The mixture density (ρ_m) and viscosity (μ_m) are calculated using the following equations [8, 9]:

$$\rho_{\mathrm{m}}=\alpha_v\rho_v+(1-\alpha_v-\alpha_g)\rho_l+\alpha_g\rho_g \tag{3}$$

$$\mu_m=\alpha_v\mu_v+(1-\alpha_v-\alpha_g)\mu_l+\alpha_g\mu_g \tag{4}$$

$$\alpha=\frac{n_b\times\frac{4}{3}\times\pi R_b^{\,3}}{1+n_b\times\frac{4}{3}\times\pi R_b^{\,3}} \tag{5}$$

Where the subscripts v,l and g represent the vapor, liquid, and gas, respectively. α is vapor volume fraction, n_b is number of bubble per volume of liquid and R_b is bubble's radius.

The $SST\ k-\omega$ turbulence model is adopted in this study, which is a blending between the $k-\omega$ model in the near-wall region and the $k-\varepsilon$ model in the far field developed by Menter[11].

Singhal et al. [9] proposed a model where the vapor mass fraction is the dependent variable in the transport equation. This formulation is given as follows:

$$\frac{\partial}{\partial t}(f_v\rho)+\nabla.\left(f_v\rho\vec{V}_v\right)=\nabla.(\nabla\Gamma f_v)+R_e-R_c \tag{6}$$

Where f_v is the vapor mass fraction, f_g is the noncandensable gases and Γ is the diffusion coefficient. The rates of mass exchange are given by the following equations:

If $p\le p_v$

$$R_e=F_{vap}\frac{\max\left(1/\sqrt{k}\right)(1-f_v-f_g)}{\sigma}\rho_l\rho_v\sqrt{\frac{2(p_v-p)}{g\rho_l}} \tag{7}$$

If $p>p_v$

$$R_c=F_{con}\frac{\max\left(1/\sqrt{k}\right)f_v}{\sigma}\rho_l\rho_v\sqrt{\frac{2(p_v-p)}{g\rho_l}} \tag{8}$$

Estimation of the local values of the turbulent pressure fluctuations as [8, 12]:

$$p_v=p_{sat}+0.5(0.39\rho k) \tag{9}$$

The second term in eq.9 from the right side (0.39ρk) is turbulent pressure fluctuation. The constant have the values F_{vap}=0.02 and F_{cond} = 0.01. The liquid-vapor mixture in this model is assumed to be compressible.

3. Validation of Computational Model

The experimental data from [6] was used for a comprehensive model validation. These experiments were conducted in a transparent quasi-two dimensional geometry, wherein the back pressure was varied to achieve different mass flow rates. To the best of our knowledge, this experimental data set is the most comprehensive in terms of two-phase information and inner nozzle flow properties. A rectangular converging channel was used with an inlet width (D_{in}) of 301 μm, outlet width (D_{out}) of 284 μm, length (L) of 1000 μm, inlet rounding radius (r) of 20 μm, and thickness of 300 μm. These dimensions correspond to an r /Rin =0.133, L/Din=3.322, which are representative of orifice in current generation diesel. Fuel temperature is 300 k and fuel injection pressure was fixed at 100 bar. Although modern diesel injector work under 1800 bar of injecting fuel, high injection pressure makes experiments very difficult and some boundaries like lack of equipment prevent injection pressure in real condition inside nozzle's

throttle. Simulation was performed in 2D condition. The grid independency was examined by three grid densities in nozzle's orifice, namely 39×20 (Grid 1), 74×44 (Grid 2) and 104×90 (Grid 3).

3.1 Boundary condition

In all parts of this simulation pressure, inlet is fixed to 100 bar and pressure outlet varies from 15 bar to 80 bar. Cavitation condition starts when pressure difference (the difference between inlet and outlet pressure) is 60 bar. Pressure difference 70 bar is threshold for initiating super cavitation which is called critical cavitation (**CC condition**) and as pressure increases 1 bar in this condition, supercavitaion will form instantaneously. Choke condition starts when pressure difference is 80bar.

The turbulence parameters that have been used in this simulation are in some situation, turbulence kinetic energy (k) and turbulence dissipation rate (ω); in other situation hydraulic diameter (D_h) and turbulence intensity (I) should be determined. Figure.1 shows the boundary condition which is used for this simulation, for the inlet and outlet boundary, pressure should be determined.

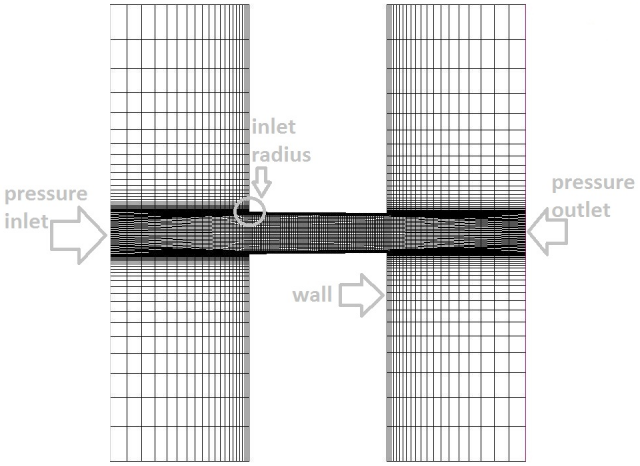

Figure .1. Nozzle's geometry when mesh density is 74×44 with zero inlet radius

Figure.2 presents velocity profiles in the transverse direction at a location 53 μm from the nozzle entrance for both cavitating (ΔP =67 bar) and noncavitating (ΔP=55 bar) conditions. With higher ΔP, higher velocities are observed. For ΔP=55 bar, the velocity peaks in the shear layer approximately 50 μm from the bottom wall, and then decreases to a minimum value at the center (y=0). Under cavitating conditions (ΔP=67 bar), a similar trend is observed, except that velocities are higher due to larger pressure difference for this case. Simulations capture these trends well except for some overprediction in the nozzle center region. Grid 1 and 3 are not able to predict velocity profile accurately, as figure 2 shows, grid 3 overpredicts velocity profile and maximum velocity at position -50 μm and 50 μm and it is not applicable for acceptable simulation. Grid 1 underestimated maximum velocity at position -50 μm and 50 μm. Grid 1 does not have an acceptable correlation with the experimental data. Simulation will be performed with **Grid 2** in the following parts because of its capability of predicting maximum velocity and near wall velocity with a similar trend in comparison with the experimental data.

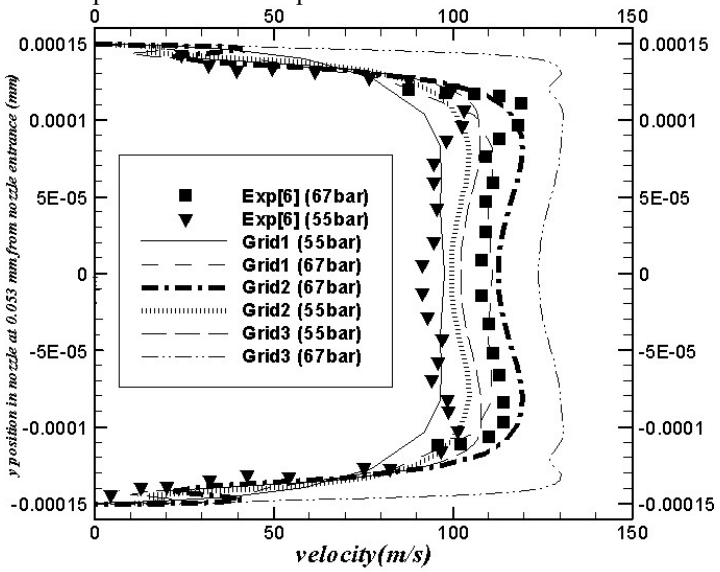

Figure .2. Predicted and measured velocity profiles at a location 53 μm from the nozzle inlet. Simulations are performed at a fixed injection pressure of 100 bar and different back pressures. Grid 1: (39×20); Grid 2: (74×44) and Grid 3 (104×90).

Figure.3 shows mass flow rate versus pressure difference. Prediction of choke condition in nozzles is very challenging but this simulation could predict mass flow rate in choke condition that have 1.9% deviation from Winklhofer et al. experiment.

Figure.4 illustrates pressure distribution profile in the simulated case at CC condition (Δp=70bar) along middle line in nozzle's throttle. Although the minimum pressure attained in the calculations is smaller than in the experiment, due to different critical condition obtained, there is good qualitative agreement. It is seen that along the line that pressure minimum appears in the zone of low pressure, recirculation is followed by pressure recovery downstream of the throttle entrance. It is observed that this simulation can predict low pressure at nozzle's entrance with acceptable accuracy. The lowest pressure near nozzle entrance region is 2.901E6. The deviation of the value which is obtained from simulation in comparison with experimental result is 8.28% at nozzle's entrance. Minimum pressure distribution in this simulation (solid line) has more accuracy in comparison with X.Margot CFD result [19] (dash line).

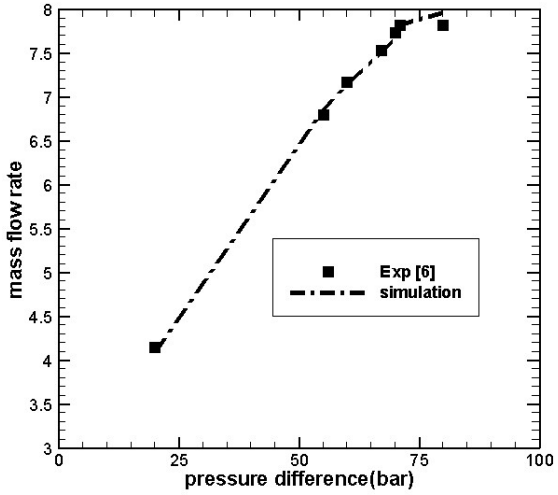

Figure .3. Predicted mass flow rate in comparison with Winklhofer et al. experiment.

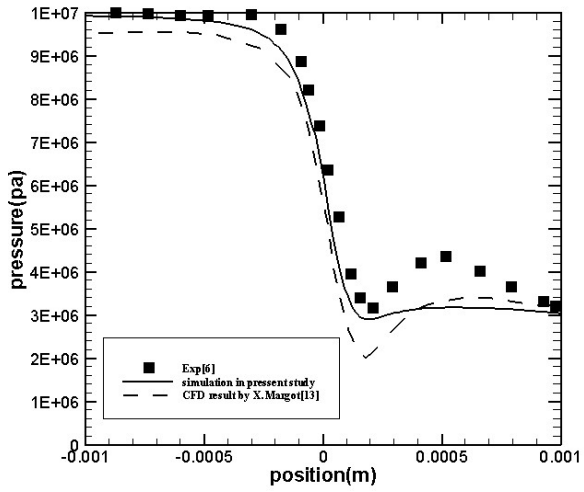

Figure .4. Predicted and Experimental pressure profile at CC condition (Δp=70bar).

4. Results and Discussion

4.1 Effect of contraction inside nozzle's orifice

Contraction among different nozzle is one the crucial parameter that affects spray process very much, the criterion utilized in this study is:

$$k(percent) = \frac{D_{in} - D_{out}}{D_{in}} \times 100 \tag{10}$$

In this part of simulation, the magnitude of D_{in} in three different simulations is 0.301mm and D_{out} values are 0.301mm (0 percent contraction), 0.284mm (5.6 percent contraction) and 0.270mm (10.3 percent contraction).

Figure.5 shows when the value of contraction varies, the critical cavitation threshold will change and as

contraction increases the value of pressure at nozzle entrance will decrease significantly and it is clear that critical cavitation condition will change.

In an experimental case (5% contraction) Winklhofer et al. (2001) reported 70 bar pressure difference for the critical cavitation condition (inlet pressure 100 bar and outlet pressure 30 bar) but as contraction increases from 5.6% to 10.3%, pressure at nozzle entrance increases and the critical cavitation condition changes.

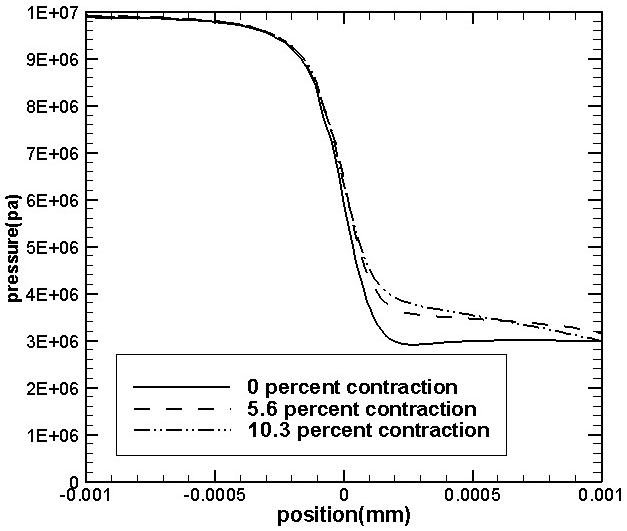

Figure.5. Predicted pressure for three different outlet diameter in nozzle's orifice (position 0 mm is nozzle's orifice entrance)

Figure 6 shows that as contraction percentage increases, the peak of velocity profile decreases but velocity in near wall region increases. Increasing velocity will decrease pressure, and critical cavitation condition will change. As contraction increases the mass flow rate ($\dot{m} = \rho A V$) will decrease (area and velocity become lower) and it is one of the disadvantages for contraction. On the other hand, increasing contraction allows us to increase injection or decrease outlet pressure without reaching the choke condition and it could be beneficial for spray process and atomization.

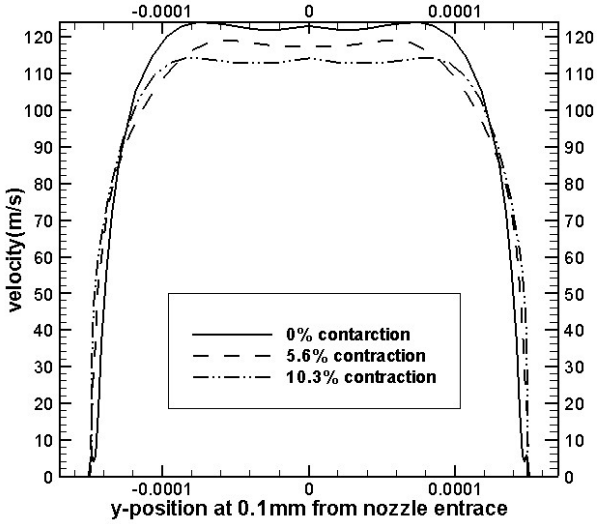

Figure .6. Velocity profile in y-position at 0.1mm from nozzle entrance with two different contractions

Figure.7 shows that different contraction percentage has no significant effect on outlet pressure, and pressure profiles are approximately similar to each other and they are in similar trend.

4.2 Discharge Coeffiecient and compressibility effect Inside Orifice

Visualization of two phase flow has been used to identify the basic flow pattern. The efficiency of the injection process is determined by the quality of the spray atomization and hydraulic resistance of nozzle, both of which affect cavitation.

The measure of the hydraulic resistance of nozzle is the discharge coefficient [14]:

$$C_d = \frac{\dot{m}_{actual}}{\dot{m}_{ideal}} \tag{11}$$

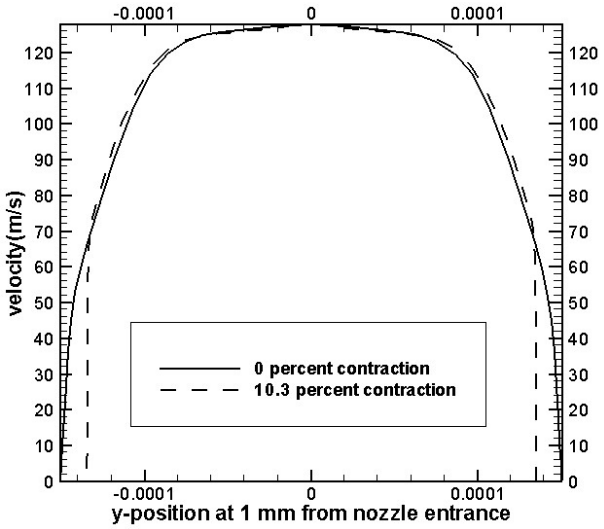

Figure .7. Velocity profile in y-position at 1mm from nozzle entrance (nozzle outlet) with two different contractions

where $\dot{m}_{actual}$ is actual mass flow rate through nozzle; and $\dot{m}_{ideal}$ is calculated as below:

$$\dot{m}_{ideal} = A_{ideal}\sqrt{2\times\rho_f\times\Delta P} \tag{12}$$

In equation (12) A_{ideal} is the cross-sectional area of the nozzle, ΔP is the pressure difference between the inlet and outlet of nozzle, ρ_f is fluid density which is chevron diesel in this simulation.

Discharge coefficient is one of the crucial parameters in diesel injector nozzle. In this stage of this study, discharge coefficient will evaluate in several injection pressures.

The three coefficients are related as:

$$C_d = C_v \times C_a \tag{13}$$

The area of contraction coefficient is defined as:

$$C_a = \frac{A_{effective}}{A_{ideal}} \tag{14}$$

Where $A_{effective}$ represents the area occupied by the liquid fuel. C_a is an important parameter to characterize cavitation, as it is recently influenced by the amount of vapor present at the nozzle exit. The Reynolds number is calculated as below:

$$\mathrm{Re} = \frac{V_{th}D_{th}\rho_{fuel}}{\mu_{fuel}} \tag{15}$$

Where D_{th} is nozzle exit diameter of the nozzle's orifice. The cavitation is often characterized in terms of global cavitation number (CN):

$$CN = \frac{\Delta P}{P_{back} - P_{vapor}} \tag{16}$$

Where P_{vapor} represents the fuel vapor pressure at the specific temperature. Properties of different fuel are listed in Table 1.

Compressible flows can be characterized by the value of Mach number [8]:

$$M = \frac{u}{c} \tag{17}$$

Here, c is speed of sound in the fluid and by defining UDF in Ansys fluent v15, it is recommended to use separated function for speed of the sound. Speed of sound is defined as below:

$$c = \left(1 - \frac{P_{cell}}{B_M}\right)\times\sqrt{\frac{B_M}{\rho_{ref}}} \tag{18}$$

In equation (18) B_M is bulk modulus for diesel fuel and ρ_{ref} is reference density of diesel fuel which is 822.7 for chevron diesel, and P_{cell} is pressure at each cell separately.

Variant density for considering the effect of compressibility is as below:

$$\rho_{new} = \frac{\rho_{ref}}{1 - \frac{P_{cell}}{B_M}} \tag{19}$$

In equation (19), ρ_{new} is new density which changes according to cell pressure. Table 1 demonstrates properties

of different fuels used in this study. As it is clear from this Table, European diesel has more density than Chevron diesel, Viscosity of European diesel is also denser than Chevron diesel. Discussing the effects of different Viscosity is not in the scope of this study, but it is important to note that effect of contraction in the previous part was investigated with European diesel and effects of discharge coefficient and nozzle entry will be investigated with Chevron diesel.

Table 1. Fuel properties at 40°C

Property	European diesel	Chevron diesel
Density(kg/m^3)	835.0	822.7
Viscosity(kg/m s)	0.0025	0.0021
Surface tension(N/m)	0.020	0.020
Vapor Pressure(pa)	1000	1000

Figure.8 shows the effect of different injection pressures and compressibility on discharge coefficient. To investigate the effect of injection pressure and compressibility on discharge coefficient, discharge coefficient versus cavitation number is plotted. In case 1, injection pressure is 1000 bar and back pressure is 1 bar ; in case 2, injection pressure is 2000 bar and back pressure is 1 bar and finally, in case 3, injection pressure is 3000 bar and back pressure is 1 bar.
Figure.8 includes 2 diagrams; the triangle symbol shows the effect of compressibility in three different injection pressures, while the square symbol shows the effect of flow with constant density in three different injection pressures. Both of these diagrams have the same trend except that the effect of compressibility discharge coefficient will increase and this event shows that in the situations which flow has high velocity, using a model with compressibility effects are necessary. For considering the effects of compressibility, a UDF[1] is also used during modelling in Ansys fluent v15. As it is clear in figure 8, by increasing pressure at inlet boundary condition, discharge coefficient will decrease and when discharge coefficient decreases, atomization will be affected. By affecting atomization, we mean that efficiency of atomization process will decrease and it is not desirable for injection cycles, but on the other hand, modern diesel engine is going toward using high pressure for reducing the time delay between each process. As a whole, using compressibility will result in more robust result but getting convergence with UDF is more difficult than usual. In this part, simulation preformed when nozzle throttle contraction is 5%. On the other hand, what can be understood from the results in figure 8 is that the slope of the line with compressibility effect is lower than the slope of the line without compressibility effect.

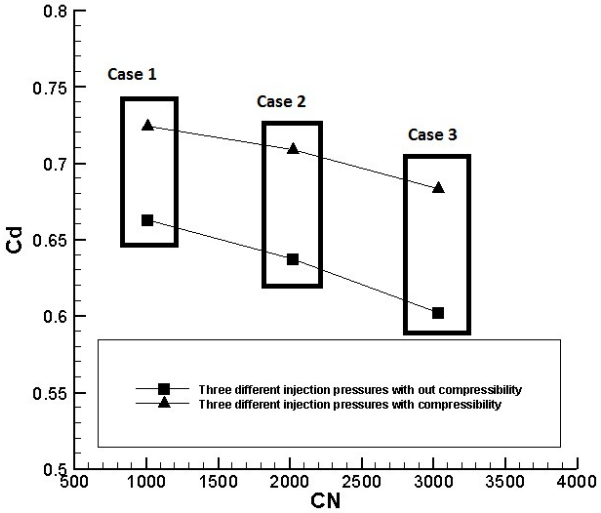

Figure.8. Discharge coefficient versus Cavitation number in three different cases

In figure.9, the effect of different discharge coefficient in three different injection pressures is investigated. As it is clear from this figure, compressibility effect the trend of these two diagram, by considering the effect of compressibility, diminishing discharge coefficient in case 3 is lower than the model with the effect of compressibility. Boundary condition in the simulation for figure 8 is the same as the boundary condition for simulation for figure 9. In addition, it is clear that for higher Re number, the flow will become turbulent and while flow is turbulent discharge coefficient will decrease significantly and it is not desirable for atomization process.
Figure 10 shows velocity profile in three different injection pressures with and without the effect of compressibility versus y-position at the middle of nozzle's orifice (50 micrometer from nozzle outlet). One of the most obvious things which is visible in this figure is that velocity increases by increasing pressure differences between the inlet and outlet of the nozzle's orifice.
As it is obvious in Figure 10, compressibility affects predicted velocity profile in every position; in near wall region this effect is more significant than other places; while considering compressibility, slope of the line which connects

[1] User Define Function

velocity in near wall region and in middle of the orifice increases and this kind of connection with higher slope is more reasonable. But, as a whole, considering the effect of compressibility, changes velocity profile and decreases it. All of the six diagrams which are in figure 10 have the same trend two by two, except in the near wall region which the values predicted with compressibility are more reasonable. The pressures which are in legend of Figure 10 are inlet pressure and in all cases outlet pressure is fixed to 1 bar (100 kpa). It can be concluded from figure 10 that by increasing injection pressure compressibility effect is going to be more significant. When injection pressure is 1000 bar, the difference between the two diagrams (with and without compressibility) is approximately 50 m/s; but when injection pressure is 3000 bar this velocity difference is approximately 100 m/s; consequently it can be said that by increasing pressure compressibility, velocity profile will be affected more than before.

Figure 11 is like figure 10 but the main difference between these two figures is that, figure 10 is the middle of the nozzle's orifice, while figure 11 is in the outlet of the nozzle's orifice. In near wall region, velocity with the effect of the compressibility, predicts more reasonable result and the slope of the line which connects velocity in near wall region and in the middle of orifice is high. The effect of compressibility decreases the predicted pressure.

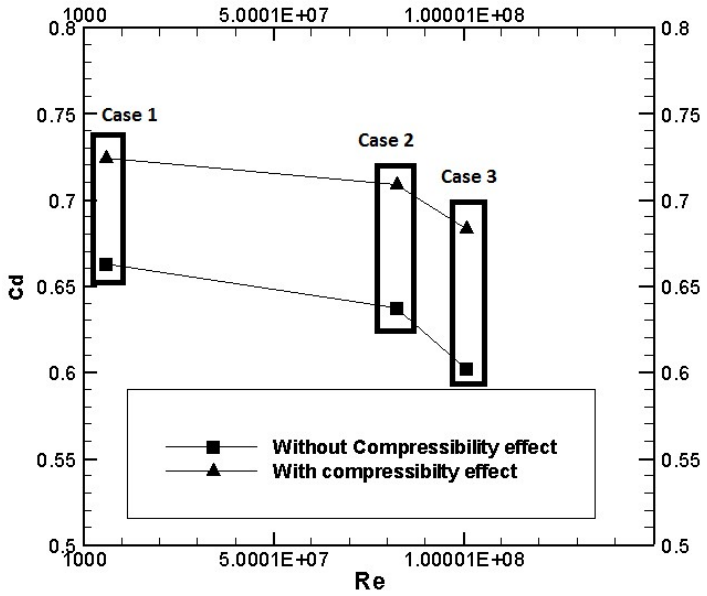

Figure.9. Discharge coefficient versus Cavitation number in three different cases

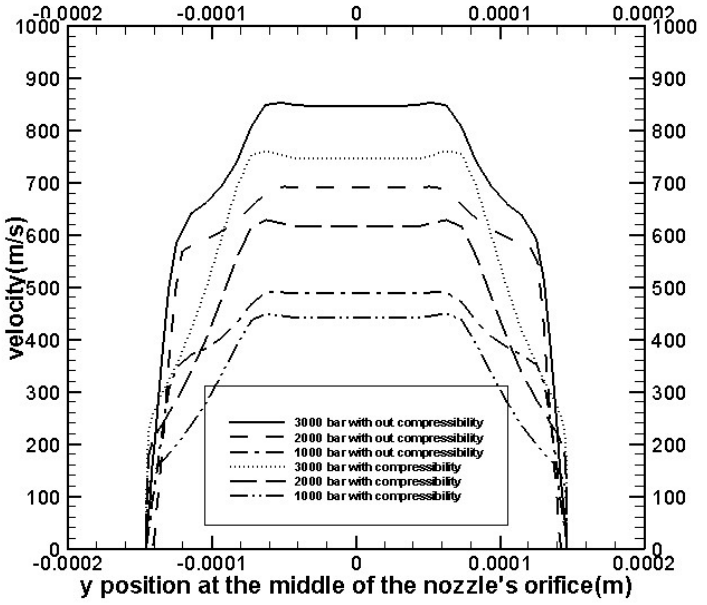

Figure.10. Velocity at the middle of the orifice in cross section area

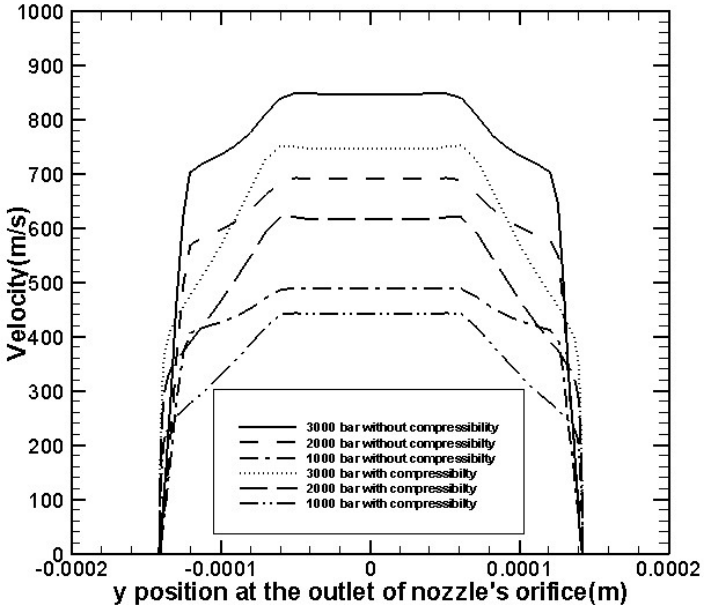

Figure.11. Velocity versus y position at the outlet of the nozzle

4.3 Shape of the orifice entry

Roundness of the orifice entry (figure 12 b) affects the recirculation flow formed at the orifice throat and the discharge coefficient of nozzle (actual mass flow rate). Rounded orifice entry reduces the length of separation region and suppresses the turbulent motion in the flow. Many experiments of cavitation flow in nozzle's orifice (Bergwerk, 1959[5]; Spike and Pennington, 1959[15]; Nurick, 1976[16]; Hiroyasu, 2000[17]; Laoonual, et al., 2001[18]; Winklhofer, et al., 2001[6]; Konig and Blessing, 2003[19]; Benajes, et al, 2004[20]) have concluded about delay (increase) in cavitation numbers for the inception and transition to super-cavitation and hydraulic flip flow caused by round shape of the nozzle's orifice entry. This is similar to the effect of beveled entry on cavitation flow.

Figure 12 shows four different orifice entries. In this section, the effect of orifice entry on mass flow rate (discharge coefficient) and velocity profile in the outlet of the nozzle's orifice will be investigated. As table 2 shows, rounded entry and beveled entry orifices have more mass flow rate, which is necessary for better performance of injectors and enhances the atomization process. Sharp entry orifices and counter bore orifices have less mass flow rates, which are not desirable for high performance atomization process and this event will decrease the whole performance of injection process in diesel injector nozzles. Simulation in this part is going to perform on nozzle's orifice without any contraction.

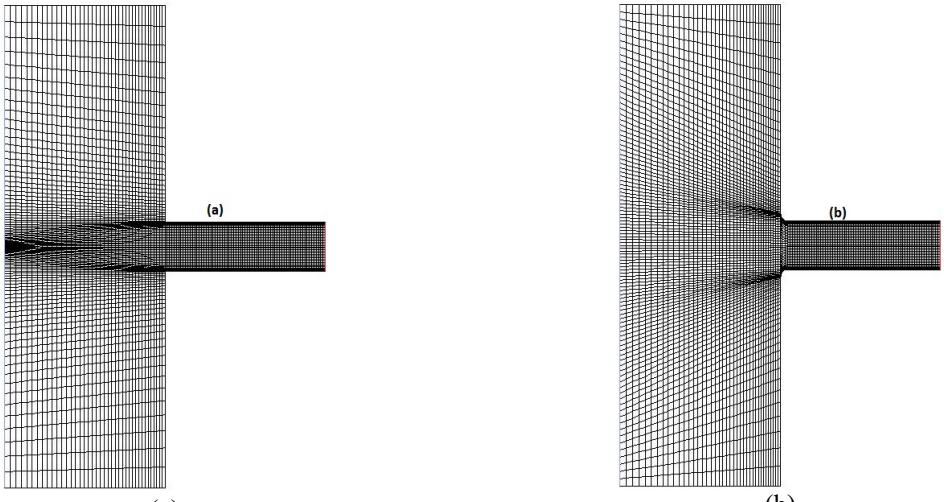

(a) (b)

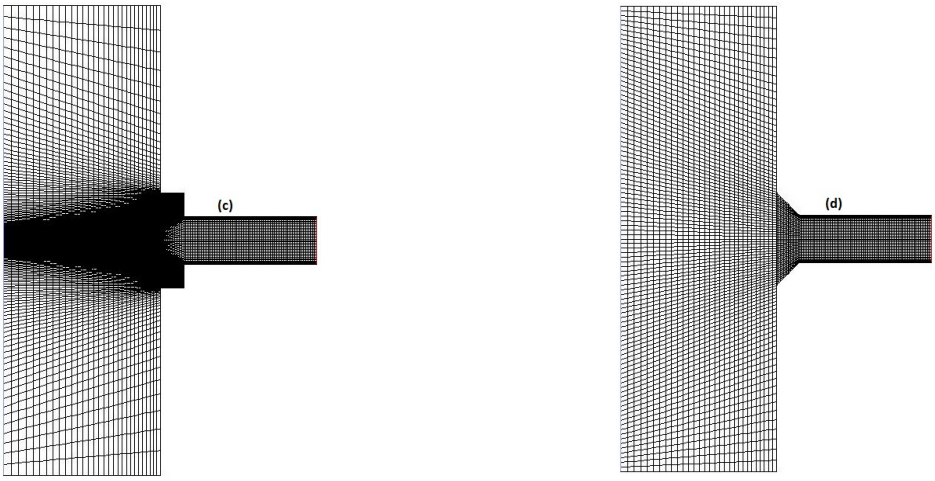

(c) (d)

Figure.12. Nozzles of different configuration entry shape, (a) - sharp entry orifice; (b) – rounded entry orifice; (c) – counter bore orifice; (d) – beveled entry orifice

Table.2. Mass flow rate with different orifice entry

Actual mas flow rate($\dot{m}$)	Kg/s
sharp entry orifice (entry number 1)	76.820
rounded entry orifice (entry number 2)	100.660
counter bore orifice (entry number 3)	79.109
beveled entry orifice (entry number 3)	102.997

Figure 13 shows velocity versus y-position inside the orifice cross section. This figure shows that entry number 3 (counter bore orifice) has a higher velocity than other entries. But entry number 3 has less mass flow rate than rounded and beveled entry orifice, which is reasonable. As it is clear, inlet in entry number 1 and 2 are sharp, which sharp inlet decreases mass flow rate although their velocity in the middle of nozzle increases. In the counter bore orifice, velocity in the near wall region is significantly lower than others and this diminishes results in lower mass flow. Using rounded entry orifice is recommended because it has a reasonable mass flow rate and high velocity together.

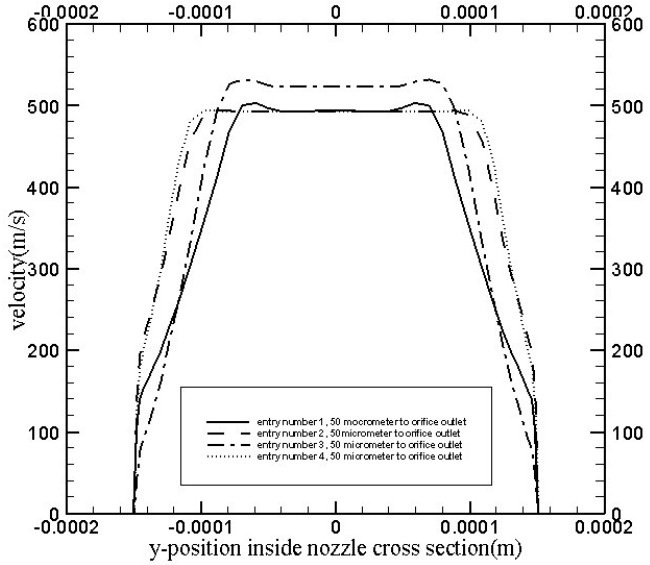

Figure.13. Velocity at the outlet of the nozzle with four different entry versus to y-position inside orifice cross section

5. Conclusion

All of the experimental data are related to Winklhofer et al (2001). Simualtion was performed with structural mesh which was implemented in Gambit meshing software. Validation was performed via several parameters like velocity profile. Predicting choke flow condition is so challenging a phenomenon that was simulated in this paper with an acceptable accuracy (1.9% deviation with experimental data). Results of the present paper are listed below:

1. Singhal et al cavitation model is very robust and can predict choke flow condition for diesel fuel inside diesel injector nozzles.
2. Contraction affects velocity profile and for lower contraction, higher velocity profile was observed. But there is not any linear formulation between contraction and velocity profile.
3. Higher injection pressure was performed in this study (1000, 2000 and 3000 bar), while the outlet pressure in this study was 1 bar; as pressure increases, velocity increases too, but the actual mass flow rate(discharge coefficient) decreases which is not desirable for high performance diesel injector nozzle.
4. Considering the effect of compressibility is very crucial and it shows that by considering compressibility, velocity decreases but in the near wall region velocity can be predicted more reasonable, because the slope of the line which connects velocity in near wall region and in the middle of the line is higher.
5. Four different nozzle's orifice entries were simulated in this study; it was shown that beveled entry orifice has the highest mass flow rate among other entries, but in this case, velocity is not high and acceptable. Sharp entry and counter bore entries have little mass flow in comparison with rounded and beveled entries. Generally, it is recommended that rounded entry be used, since it has more mass flow rate and more velocity together.

Nomenclature

ρ_m	Mixture density [kg/m^3]
μ_m	Mixture dynamic vicosity [N·s/m^2]
ρ_l	Density of liquid [kg/m^3]
μ_l	Dynamic viscosity of liquid [N·s/m^2]
ρ_v	Density of vapour [kg/m^3]
μ_v	Dynamic viscosity of vapour [N·s/m^2]
α	Vapour volume fraction [dimentionless]
α_g	Vapour volume fraction for gas phase [dimentionless]
α_l	Vapour volume fraction for vapour phase [dimentionless]
v	Velocity[m/s]
M	Mach number
c	Speed of sound
P_{cell}	Pressure at each cell
nb	Number of bubbles [dimentionless]
Rb	Radius of bubble[m]
P	Pressure [pascal or ba]
Pv	Vaporization pressure [pascal or bar]
Γ	Diffusion coeffient
fv	Vapor mass fraction
fg	Noncondensable gases
K	Temperature[K]
k	Turbulent kinetic energy[m^2/s^2]
ω	Turbulent dissipation rate[1/s]
I	Turbulent intensity [dimentionless]
u	Liuid velocity
B_M	Bulk modulus
ρ_{ref}	Reference density
ρ_{new}	Variable density according to pressure and sound velocity

References

[1] PHD thesis. Daniele Liuzzi, 2012." Two-Phase Cavitation Modelling". UNIVERSITY OF ROME - LA SAPIENZA -

[2] Faeth, G. M. and Hsiang, L-P and Wu, P-K, 1995. "Structure and Breakup Properties of Sprays". International Journal of Multiphase Flow, 21, pp. 99–127.

[3] Sato, K. and Saito, Y. (2001) Unstable cavitation behaviour in circular-cylindrical orifice flow. Proc. of the 4th Int. Symposium on Cavitation: CAV2001, 8 p.

[4] Stinebring, D.R., Billet, M.L., Lindau, J.W. and Kunz, R.F. (2001) Developed cavitation-cavity dynamics. VKI Lecture Series on Supercavitating Flows. VKI Press, Brussels, 2001, 20 p.

[5] Bergwerk, W. (1959) Flow Pattern in Diesel Nozzle Spray Holes. Proc. Inst. Mech Engrs., 1959, Vol.173, pp. 655 – 660.

[6] Winklhofer, E., Kull, E., Kelz, E., Morozov, A. (2001) Comprehensive hydraulic and flow field documentation in modl throttle experiments under cavitation conditions. Proceedings of the ILASS-Europe Conference, Zurich, 2-6 September, 2001, pp. 574 – 579.

[7] PHD thesis.SERGEY MARTYNOV (2005)." Numerical Simulation of the Cavitation Process in Diesel Fuel Injectors".

[8] Ansys Fluent v14 Documentation.

[9] Singhal, A.K., Athavale, M.M., Li, H., Jiang Yu (2002) Mathematical basis and validation of the full cavitation model. Tr. ASME, J. Fluid Eng., Vol.124, pp. 617 – 624.
[10] Han, J. S., Lu, P. H., Xie, X. B., Lai, M. C., and Henein, N. A., 2002, "Investigation of Diesel Spray Break Up and Development for Different Nozzle Geometries," SAE Paper No. 2002-01-2775.
[11] Menter F R. Two-Equation eddy-viscosity turbulence models for engineering applications [J]. AIAA Journal, 1994, 32(8): 1598-1605.
[12] Hinze, J. O., 1975, Turbulence, 2nd Ed. McGraw Hill, New York.
[13] X.margot, S.Hoyas, A.Gil,,S.Patouna, 2012."Numerical modelling of cavitation:validation and parametric studies". Engineering application of computional fluid mechanics Vol 6, No. 1, pp. 15-24.
[14] Naber, J. D., and Siebers, D. L., 1996, "Effects of Gas Density and Vaporization on Penetration and Dispersion of Diesel Sprays," SAE Paper No. 960034.
[15] Spikes, R.H., and Pennington, G.A. (1959) Discharge coefficient of small submerged orifices. Proc. Inst. Mech. Engineers, pp. 661 – 674.
[16] Nurick, W.H. (1976) Orifice cavitation and its effect on spray mixing. J. Fluids Engng., 98, pp. 681 – 689.
[17] Hiroyasu, h. (2000) Spray breakup mechanism from the hole-type nozzle and its applications. Atomization and Sprays, Vol.10, pp. 511-527.
[18] Laoonual, Y., Yule, A.J, and Walmsley, S.J. (2001). Internal fluid flow and spray visualization for a large-scale VCO orifice injector nozzle. ILASS-Europe 2001, Zurich 2-6 September, 2001. 6 p.
[19] Blessing, M., Konig, G., Kruger, C., Michels, U., and Schwarz, V. (2003) Analysis of flow and cavitation phenomena in Diesel injection nozzles and its effects on spray and mixture formation. SAE paper 2003-01-1358, pp. 29 – 39.
[20] Benajes, J., Pastor, J.V., Payri, R. and Plazas, A.H. (2004) Experiments for the different values of K-factor. J. Fuids Engineering, Vol.126, p. 63.